Characterization of the Extracellular Ligand-Binding Domain of the Type II Activin Receptor†

Jason Greenwald,‡,§ Vincent Le,‡,§ Anne Corrigan,|| Wolfgang Fischer,|| Elizabeth Komives,§ Wylie Vale,|| and Senyon Choe*,‡

Structural Biology Laboratory and Clayton Foundation Laboratories for Peptide Biology, The Salk Institute, La Jolla, California 92037, and Department of Chemistry and Biochemisty, University of California San Diego, La Jolla, California 92093

Received August 11, 1998; Revised Manuscript Received September 23, 1998

ABSTRACT: The binding of a ligand to cell surface receptors initiates a cascade of intracellular signals that generate responses to the external stimuli. Thus, this event plays a pivotal role in the mechanism of transmembrane signaling. Activin is a member of a cytokine family that is involved in diverse biological processes. To study the structural basis that underlies the transmembrane signaling mechanism, we have overexpressed the soluble extracellular domain of the type II activin receptor from mouse (ActRII-ECD). We used the methylotrophic yeast *Pichia pastoris* as an expression host to produce a large quantity of ActRII-ECD. Expression was carried out in a fermentor with a typical yield of 10 mg of pure ActRII-ECD from a liter of growth media. Biological function was confirmed by the ability to decrease the activin-stimulated release of FSH from cultured rat pituitary cells in addition to several activin-binding assays, including native gel shift and chemical cross-linking. The glycosylation on ActRII-ECD was shown to be dispensable for high-affinity activin binding, and nonnatural sugars from the yeast expression host did not interfere with binding, indicating that the binding of activin is not sensitive to the environment near the two positions of N-linked glycosylation. Analytical ultracentrifugation of the complex between activin A and ActRII-ECD reveals that two receptors associate with one activin A dimer, consistent with results from chemical cross-linking experiments.

Living cells are constantly receiving instructions from other cells. These signals, which are often in the form of a protein messenger, instruct the cell to grow, remain quiescent, differentiate, or die. Such complex signaling pathways that are connected in a multidimensional manner are all set into motion by the recognition and assembly of ligand and receptor molecules at the cell surface. The structural basis for such a signaling mechanism is, however, not well understood. An accurate knowledge of one such transmembrane signaling mechanism will provide the foundation on which a more complex physiological phenomenon, in which there are multiple ligand and receptor complexes acting in concert, can be understood.

Activins belong to the TGFβ[1] superfamily of growth factors and can affect a broad range of cellular processes such as cell division (*1*, *2*), differentiation (*3*), and pattern formation during embryogenesis (*4*, *5*). Activins were originally identified as proteins which stimulate the production of FSH by the anterior pituitary gland (*6*). The physiological action of activin is antagonized by inhibin, a related protein that inhibits the prodution of FSH (*7*, *8*). Activins are disulfide-linked homo- and heterodimers of related β subunits. β_A and β_B combine to form three different types of activin: A ($\beta_A\beta_A$), B ($\beta_B\beta_B$), and AB ($\beta_A\beta_B$). Three new β chains, β_C, β_D, and β_E, have recently been identified, forming a new subclass of activins based on their sequence similarity and limited expression pattern (*9*−*12*); however, their biological roles are still not well characterized. A slightly larger and more distantly related chain, called α, can form heterodimers with the β chains to form inhibin A ($\alpha\beta_A$) and inhibin B ($\alpha\beta_B$). The sequence similarity between β and α chains and subunits of TGFβ suggests that the structure of activin is similar to that of TGFβ, for which the crystal structure has been elucidated (*13*, *14*).

Two kinds of receptors, type I and type II, are required to mediate the cellular responses of the TGFβ superfamily members (*15*, *16*). Both are single transmembrane receptors with intracellular serine/threonine kinase domains (*17*). In addition to the serine kinase, the cytoplasmic domain of the type I receptor contains a ∼30 residue segment called the GS domain which is located between the transmembrane and kinase domains (*18*). The GS domain has several conserved Gly, Ser, and Thr residues of which the Ser and Thr residues are targets for phosphorylation by the type II receptor and

† This work was supported by NIH Grant HD13527. J.G. is a Howard Hughes Medical Institute Predoctoral Fellow and Markey Fellow. S.C. is a recipient of a Klingenstein Fellowship Award in Neuroscience.

* Corresponding author. E-mail: choe@sbl.salk.edu.

‡ Structural Biology Laboratory, The Salk Institute.

§ Department of Chemistry and Biochemistry, University of California San Diego.

|| Clayton Foundation Laboratories for Peptide Biology, The Salk Institute.

[1] Abbreviations: ECD, extracellular domain; ActRI, type I activin receptor; ActRII, type II activin receptor; TGFβ, transforming growth factor β; TGFβRII, type II transforming growth factor β receptor; FSH, follicle stimulating hormone; SDS−PAGE, sodium dodecyl sulfate−polyacrylamide gel electrophoresis; DSS, disuccinimidyl suberate.

10.1021/bi981939o CCC: $15.00
Published on Web 10/31/1998

are important for the activation of the type I receptor (*19*, *20*). The type II receptor is capable of binding to the ligand, and has a constitutively active kinase; however, it cannot propagate a signal without the type I receptor. On the other hand, the type I receptor can only form a complex with ligand that is already bound to the type II receptor (*21*).

The formation of the signaling complex, which consists of ActRI, ActRII, and activin, causes transphosphorylation of ActRI by ActRII, thereby activating the kinase domain of ActRI which phosphorylates downstream components to propagate the signal. This mechanism of receptor heterodimerization plays an important role in creating diverse and tunable responses to complex extracellular simuli. An example that demonstrates the complexity of activin-mediated signaling is the dose-dependent response in *Xenopus* embryos. *Xenopus* blastomeres respond differently to a 1.5-fold difference in activin stimulation, at one dose forming muscle and another forming notochord (*5*). This exquisitely tuned signal response, for which a mechanism is not known, is necessary for the development of multicellular eukaryotes. The structural basis for this type of signaling mechanism involving more than one target receptor is the ultimate focus of our study.

In the present study, we describe the overexpression, purification, and preliminary characterization of the extracellular domain of the type II activin receptor from mouse (ActRII-ECD). The mouse and human ActRII-ECDs differ only at 2 out of 116 residues. We demonstrate that ActRII-ECD is monomeric in solution, and that it is capable of competing with ActRII, thereby acting as an inhibitor of activin signaling. We also show that the activin A/ActRII-ECD complex in solution consists of one dimeric activin A with two chains of ActRII-ECD. Finally, we demonstrate that glycosylation is not crucial for ligand/receptor recognition and binding.

EXPERIMENTAL PROCEDURES

Media and Solutions. YPD: 10% Bacto yeast extract, 20% Bacto peptone, 2% glucose. SED: 1 M sorbitol, 25 mM EDTA, 50 mM DTT. SCE: 1 M sorbitol, 1 mM EDTA, 10 mM citrate, pH 5.8. CaS: 1 M sorbitol, 10 mM Tris, pH 7.5, 10 mM $CaCl_2$. PEG solution: 20% polyethylene glycol 3350, 10 mM Tris, pH 7.5, 10 mM $CaCl_2$. SOS: 1 M sorbitol, 33% YPD media, 10 mM $CaCl_2$. 10× YNB: 34 g of yeast nitrogen base without amino acids and $(NH_4)_2SO_4$, 100 g of $(NH_4)_2SO_4$. RD Top Agar: 1 M sorbitol, 1% agar, 2% glucose, 1× YNB, 2 μg/mL biotin. RDB plates: 0.6 M KCl, 2% agar, 2% glucose, 1x YNB, 0.4 μg/mL biotin. MD plates: 2% agar, 1x YNB, 0.4 μg/mL biotin, 2% glucose. BMGY: 1x YNB, 1% glycerol, 1% casamino acids, 0.4 μg/mL biotin. BMMY: 1x YNB, 1% methanol, 1% casamino acids, 0.4 μg/mL biotin. PTM4 salts (per liter): 2 g of $CuSO_4 \cdot 5H_2O$, 80 mg of NaI, 3 g of $MnSO_4 \cdot H_2O$, 200 mg of $NaMoO_4 \cdot 2H_2O$, 20 mg of boric acid, 500 mg of $CoCl_2$, 7 g of $ZnCl_2$, 22 g of $FeSO_4 \cdot 7H_2O$, 200 mg of biotin, 1 mL of sulfuric acid. Basal salts medium (per liter): 13.3 mL of 85% phosphoric acid, 1.8 g of $CaSO_4 \cdot 2H_2O$, 14.3 g of K_2SO_4, 11.7 g of $MgSO_4 \cdot 7H_2O$, 3.9 g of KOH, 40 mL of glycerol.

Vector Construction. ActRII-ECD was expressed in *Pichia pastoris* under the control of the alcohol oxidase (AOX) promoter. The gene encoding mouse ActRII-ECD was cloned into the *P. pastoris* expression vector pPIC9K (Invitrogen) using two oligonucleotides (5′gccgagtggccatatggctatacttggcaga3′ and 5′gtggtggtgctcgaggggtggcttcggtg3′) designed to amplify the region of the ActRII gene that encodes from the signal cleavage site to the N-terminus of the transmembrane segment. This PCR product was cloned into pET21a (Novagen) at the *Nde*I and *Xho*I restriction enzyme sites which added a 6-His tag to the C-terminus. After the sequence of the new construct was verified, the gene encoding the ActRII-ECD and the His tag was subcloned into pPIC9K-TM45 using a new 3′ PCR primer (5′cgcggccgccctaggagccggatctcagtgg3′). The PCR product was cloned into pPIC9K-TM45 at the *Nde*I and *Avr*II sites. Figure 1A shows the final pPIC9K-ActRII-ECD construct which was used in the transformation of *P. pastoris*.

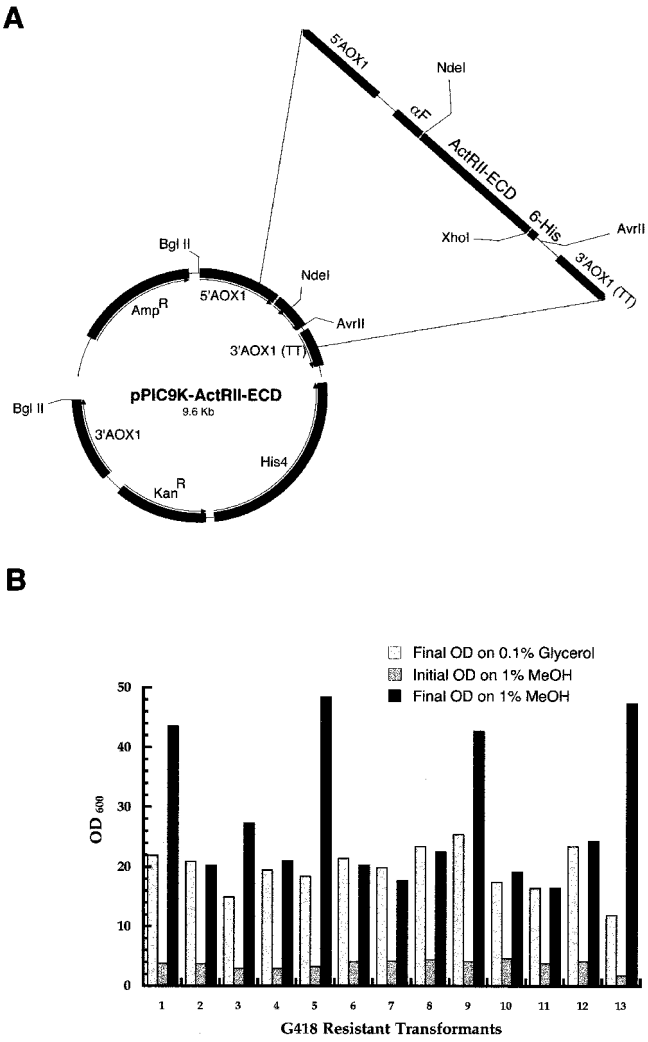

FIGURE 1: (A) Schematic representation of the pPIC9K vector that was used to express ActRII-ECD with a close-up around the cloning region. The vector contains the following elements: 5′AOX1 promoter region, α-factor secretion signal, ActRII-ECD, 6-histidine tag, 3′AOX1 transcription termination region (TT), His4 ORF, kanamycin resistance gene, 3′AOX1 fragment, ampicillin resistance gene. (B) To identify Mut^+ colonies for expression in the fermentor, G418 colonies were grown for 24 h in 0.1% glycerol BMGY, spun down, and then grown for 24 h in 1% methanol BMMY. A plot of the OD_{600} for 13 G418 resistant clones reveals which are Mut^+ by their higher cell density after growth on methanol.

Spheroplast Transformation. We used the SMD1168 strain of *P. pastoris* for transformation. SMD1168 is a $his4^-$

pep4$^-$ strain that is deficient in protease A, resulting in a deficiency in carboxypeptidase Y and protease B1. This strain is also lacking a functional His4 gene, which is contained in the pPIC9K expression vector. His$^+$ transformants grow on media without histidine, providing a simple selection for colonies that contain the vector. Spheroplast transformation was the only method which yielded multiple copy inserts of the pPIC9K-ActRII-ECD vector. The DNA was linearized by digestion with *Bgl*II and then purified and concentrated with the Geneclean kit (Bio 101 Inc.). Spheroplast transformation was carried out essentially as described (*22*) with some modifications (*23*). Specifically, SMD1168 cells were grown in 200 mL of YPD to an A_{600} of 0.2−0.3, and harvested by centrifugation at 1500*g*. The cells were washed and centrifuged sequentially with 20 mL of H_2O, SED, and 1 M sorbitol. The cells were then resuspended in 20 mL of SCE with 15 μL of zymolase (Z-70 ICN, 3 mg/mL), and incubated at 30 °C for 30 min. The spheroplasts were harvested at 750*g* and washed sequentially with 20 mL of 1 M sorbitol and CaS. The spheroplasts were resuspended in 400 μL of CaS; 200 μL of spheroplasts was incubated with 10 μg of linearized DNA for 10 min at room temperature. One milliliter of PEG solution was added to the cells and allowed to incubate another 10 min. The cells were collected by centrifugation at 750*g* in a microcentrifuge, and the PEG was carefully removed. The pellet was resuspended in 150 μL of SOS and incubated at room temperature for 20 min. The cells were diluted with 850 μL of 1 M sorbitol and then added to 30 mL of RD Top Agar prewarmed at 45 °C, and then poured onto three RDB plates. The plates were incubated for 5 days at 30 °C. The top agar was scraped off of the plates and pooled into one 50 mL screw cap tube. The tube was filled with sterile water and vortexed thoroughly to remove the cells from the agar. The cells were filtered through several layers of sterile cheesecloth and then centrifuged. The cells were resuspended in YPD with 15% glycerol and stored at −70 °C.

Selection of Multiple Copy Inserts. Cells from the his$^+$ transformant pool were spread on MD plates at an appropriate dilution to give between 20 and 100 colonies per plate. These plates were incubated at 30 °C for 4 days. The colonies were replica-plated onto YPD plates which contained 2 g/L G418 (Geneticin, Gibco BRL). After 2 days, about 10% of the plated colonies had grown, and these were presumed to have at least 5 copies of the kanamycin resitance gene (*24*).

Selection of Mut$^+$ Transformants. The transformation with pPIC9K results in a number of different phenotypes depending on the points of recombination into the yeast genome. Clones which have had one of their alcohol oxidase genes disrupted will not grow as quickly on methanol and are termed "methanol utilization slow" (Mut^s). We found that Mut$^+$ clones are better suited for fermentation and therefore designed a screen for this phenotype. This screen also provided a means to identify clones that produced the most recombinant protein. G418 resistant colonies were grown in BMGY with 0.1% glycerol at 30 °C for 24 h. The cells were spun down and resuspended at an A_{600} near 2 in BMMY and grown for another 24 h. The final OD of the cultures was used to determine the phenotype of the clone. Mut^s clones reached a final OD between 17 and 24, whereas Mut$^+$ clones usually grew to at least 35 and often to 50 OD units. (Figure 1B). The medium from these test cultures was used in a Western blot to select a clone that produces the highest level of expression.

Native Gel Electrophoresis. The gel matrix consists of 4.5% acrylamide, 0.12% bis(acrylamide), and 375 mM Tris, pH 8.8. The electrophoresis buffer is 25 mM Tris, 192 mM glycine, pH 8.8. The ActRII-ECD and activin were allowed 15 min to form a complex before addition of a 6× loading buffer which contains 30% glycerol and bromophenol blue. Gels were run at 20 mA for about 1 h.

Enzymatic Deglycoslyation. The mannose oligosaccharides were removed by digestion with endoglycosidase H (Glyko), which cleaves between the two *N*-acetylglucosamines. Only 0.1 unit of enzyme was required to digest 10 mg of ActRII-ECD at 5 mg/mL in 12 h. One unit is defined as the amount of enzyme required to catalyze the release of N-linked oligosaccharides from 60 μmol of denatured ribonuclease B in 1 h at 37 °C, pH 5.5. The reactions were carried out in 50 mM $NaPO_4$, pH 5.5 at 37 °C. The reaction was monitored by SDS−PAGE and was stopped by purification on a Superdex 75 gel filtration column (Pharmacia).

Chemical Cross-Linking. Activin (^{125}I-labeled, 6×10^5 cpm) was incubated with 200 ng of ActRII-ECD in 10 mL of HEPES buffer (50 mM, pH 7.5) at 37 °C. After 30 min, the mixture was allowed to cool to RT, and 1 μL of disuccinimidyl suberate (DSS, 2 mg/mL) in DMSO was added. The reaction was stopped after 60 min by addition of nonreducing SDS sample buffer. The sample was then resolved on a 15% SDS−PAGE gel. Radioactive bands were visualized by exposure of the dried gel to X-ray film.

Solid-Phase Binding Assay. ActRII-ECD preparations were bound to the wells of an Immulon-4 microtiter plate overnight at 4 °C (100 ng/well). Residual binding sites were blocked with 0.5% poly(vinylpyrrolidone) and 0.5% gelatin in Tris-buffered saline (TBS). The wells were washed 3 times with binding buffer [HDB (137 mM NaCl, 5 mM KCl, 0.7 mM Na_2HPO_4, 25 mM HEPES, 100 μg/mL gentamycin, pH 7.4) supplemented with 5 mM $MgSO_4$, 1.6 mM $CaCl_2$, 1 mg/mL bovine serum albumin]. A premixed solution containing a constant amount of ^{125}I-labeled activin A and varying amounts of nonlabeled activin A as a displacer was added to the wells in triplicate. After 1 h incubation at room temperature, the solution was aspirated, and the wells were washed with 250 μL of ice-cold binding buffer. The wells were then counted for radioactivity. Displacement data were analyzed using the program Prism (version 2.0). Affinities were determined as EC_{50} values.

FSH Assay. Anterior pituitary glands from male Sprague−Dawley rats were dissociated by collagenase and plated (0.15×10^6 cells/well in 48-well plates) in medium containing 2% fetal bovine serum. Three days after plating, the cells were washed twice with fresh medium, and the treatments were initiated in triplicate for 72 h. FSH was measured using radioimmunoassay kits provided by Dr. A. F. Parlow of the National Hormone and Pituitary Program of NIDDK.

Analytical Ultracentrifugation. Equilibrium analytical ultracentrifugation was carried out at 23 °C (Beckman Optima XL-I), and the data were analyzed using the WinNONLIN software (*25*). The data were fit to an equation for a single nonassociating species or to a two-species equilibrium association, but the two-species fit did not

improve significantly over the single-species fit. The equation for the single species is $f(r) = A \exp[\sigma(r^2/2 - r_o^2/2)] + C$, where r is the radius, r_o is the radius at the meniscus, and σ is the reduced effective molecular weight. $\sigma = [M\omega^2(1 - \nu\rho)/RT]$, where M is the molecular weight, ω is the angular velocity, ν is the partial specific volume, ρ is the density, R is the gas constant, and T is the absolute temperature. Data were collected on each sample at three concentrations (ranging between 0.1 and 0.8 mg/mL) and at two speeds, and the σ was fit globally to all six data sets.

Growth in Fermentor Vessel. An overnight culture of 200 mL of BMGY at an OD of 20−50 was used to innoculate 3.5 L of Basal salts medium with 14 mL of PTM4 salts in a sterile 5 L fermentor vessel. The pH of the media was maintained at 5.0 throughout the run by a NH_4OH feed. The yeast were grown at 30 °C, 400 rpm agitation, with aeration and oxygen feed to keep the dissolved oxygen (DO) at or above 40 until the glycerol was consumed, at which point the wet cell weight (wcw) was around 110 g/L. After the DO had risen above 60, indicating that the cells had stopped consuming glycerol, a feed of 50% glycerol with 12 mL/L PTM4 salts was started at a flow of 40 mL/h, and the agitation was increased to 900 rpm. The glycerol feed was continued for about 20 h at which point the wcw was near 300 g/L. A 50% methanol feed with 12 mL/L PTM4 salts was started at the minimum flow rate for the fermentor and steadily increased over a period of 6 h to a rate of 20 mL/h. The methanol feed continued at this rate for 24 h. The cells were centrifuged at 10000*g* for 45 min, and the supernatant was either frozen at −20 °C or used immediately for purification.

RESULTS

Expression of ActRII-ECD. Our initial attempts at growing *P. pastoris* in a fermentor were based on reported parameters (*26*). It was not difficult to produce hundreds of milligrams of ActRII-ECD; however, to get the highest yield of properly folded protein, many parameters had to be optimized. The factors which most affected the yield of properly folded ActRII-ECD were the rate of the methanol feed during induction and the length of the induction. These yeast had tremendous growth rates on glycerol or methanol, and a 4 L fermentation culture could easily consume 500 mL of methanol in 24 h. Although they were utilizing this much methanol, they were making primarily misfolded ActRII-ECD. Eventually a slower induction rate was found to yield a higher level of properly folded ActRII-ECD. The length of the induction was critical because if it was too long then the yeast began to die and release proteases which decreased the yield. The protocol described under Experimental Procedures yielded 200 mg of ActRII-ECD from a 4 L fermentation, of which ∼40 mg after purification was properly folded and was able to bind to activin.

Purification of ActRII-ECD. ActRII-ECD was secreted to the media by a clone of *P. pastoris* which contained the ActRII-ECD gene fused to the α factor signal peptide. The initial purification was carried out by nickel affinity chromatography which concentrated the protein to a manageable volume and separated out most of the other extracellular proteins. After centrifugation, 1 M Tris was added to the media to a final concentration of 50 mM, and then 1 M NaOH was added until the pH stabilized at around 8. The change in pH caused some salt precipitation, and this in turn caused the pH to decrease. After the precipitate settled, the media were centrifuged at 10000*g* and, 5 mL of nickel NTA resin (Qiagen) was added per liter of media. The media were stirred slowly with the resin for 12 h, and then poured into a column. The resin was washed with 2 column volumes of 20 mM Tris, 150 mM NaCl, 5 mM imidazole, pH 8. The ActRII-ECD was eluted with 200 mM imidazole in the same buffer. The eluted protein was concentrated with a Centricon 10 (Amicon) and loaded onto a Superdex75 16/60 gel filtration column (Pharmacia) equilibrated in 20 mM Tris, 150 mM NaCl.

The two main peaks of the chromatogram (Figure 2A) correspond to different aggregation states of ActRII-ECD. The larger peak is misfolded ActRII-ECD and probably contains some disulfide-linked dimers. The smaller component which runs at approximately 29 kDa on SDS−PAGE is a monomeric form of the receptor. The aggregated fraction did not display any binding to activin A on a native gel, whereas the monomeric species was fully competent to bind activin A as measured on a native gel and by gel filtration (Figure 2D).

Deglycoslyation and Proteolysis of ActRII-ECD. To test whether a deglycosylated form of the ActRII-ECD could bind to activin, the high-mannose polysaccharides were removed by digestion with endoglycosidase H (Figure 2E). The deglycosylated protein (ActRII-dg) was still able to form a stable complex with activin A (Figure 3B). The ActRII-dg was a more homogeneous species as visualized by SDS−PAGE, whereas the glycosylation caused ActRII-ECD to run as a diffuse band (Figure 2E).

To probe the subdomain structure of ActRII-ECD, we screened several commercially available proteases for cutting sites. ActRII-ECD turned out to be quite stable to many proteases including trypsin, which did not significantly cut at a 1:20 weight ratio (trypsin:ActRII-ECD) even after 12 h at room temperature. Endoproteinase Glu-C (EndoC) cleaved after Glu 102, removing the 14 C-terminal residues which included the His tag (Figure 2E). The cleavage site was determined by a combination of mass spectrometry and N-terminal sequencing. The EndoC-treated ActRII-dg is referred to as ActRIIΔ14.

Activity and Binding Assays. The results of the native gel showed that activin A was able to form a stable complex with three distinct forms of the receptor (Figure 3). The mobility of the complex at pH 8.8 was only slightly less than that of the free receptor, indicating that there is not a large difference in the p*I* between ActRII-ECD and its complex with activin A. We also ran native gels of ActRIIΔ14 and its complex with activin A (Figure 3C), and in this case, the complex has a similar mobility to the complex with ActRII-ECD and ActRII-dg, but ActRIIΔ14 alone was moving with the solvent front. The increased mobility is due to the decreased p*I* that resulted from the removal of the C-terminal residues, in which the 6-His tag is contained.

ActRII-ECD and ActRII-dg were tested for activin binding by a displacement assay using activin A as a diplacer and immobilized receptor on an ELISA plate. The affinities (EC_{50}) were 1.5 nM and 7.8 nM for the glycosylated and the deglycosylated receptor, respectively (results to be

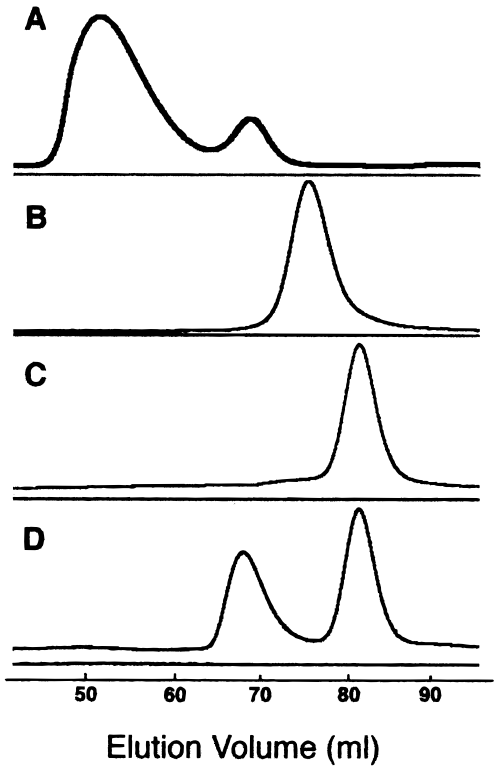

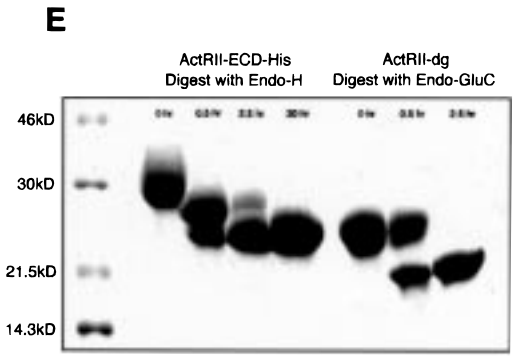

FIGURE 2: Gel filtration (Superdex 75, Phamacia) chromatograms and SDS−PAGE at different stages of ActRII-ECD purification and characterization. The *y* axis is absorbance at 280 nm on an arbitrary scale. (A) Eluted protein from the nickel column which contains a large misfolded peak and a smaller active peak (ActRII-ECD). (B) After treatment of ActRII-ECD with endoglycosidase H to remove the mannose (ActRII-dg). (C) After treatment of ActRII-dg with endoproteinase Glu-C (ActRIIΔ14). (D) Injected mixture of activin A and excess ActRIIΔ14. The peak corrosponding to the larger species is the complex between activin and ActRIIΔ14. Molecular mass markers of 150, 66, 43, 29, 12.4, and 6.5 kDa eluted at 49.1, 54.8, 62.1, 70.1, 80.6, and 93.2 mL, respectively. (E) SDS−PAGE of ActRII-ECD showing the cleavage with endoglycosidase H (Endo-H) to yield ActRII-dg and then with endoproteinase GluC (Endo-GluC) to yield ActRIIΔ14.

published elsewhere). We also measured the effect of ActRII-dg on cultured rat pituitary cells in the presence of activin. ActRII-dg was able to block activin-stimulated release of FSH from basal levels of activin and from additional activin A. ActRII-dg at 10 μg/mL was sufficient to decrease the FSH release by half in the presence of up to 10 ng/mL activin A (Figure 4). At all doses of ActRII-dg, from 0.4 to 10 μg/mL, the amount of FSH realease was lessened as the dose of ActRII-dg was increased. This indicates that the soluble ActRII-ECD is an inhibitor of

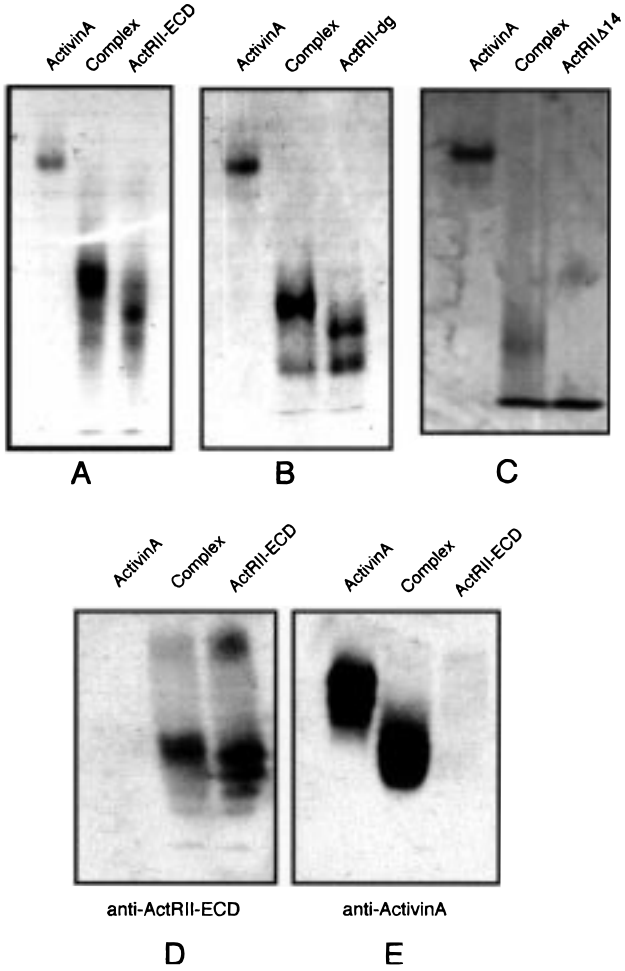

FIGURE 3: Native gels of activin A and ActRII-ECD alone and in complex with each other. Panels A, B, and C were visualized by Coomassie staining. Panels D and E were visualized by Western blot using antibodies to either ActRII-ECD or activin A and the ECL kit from Amersham.

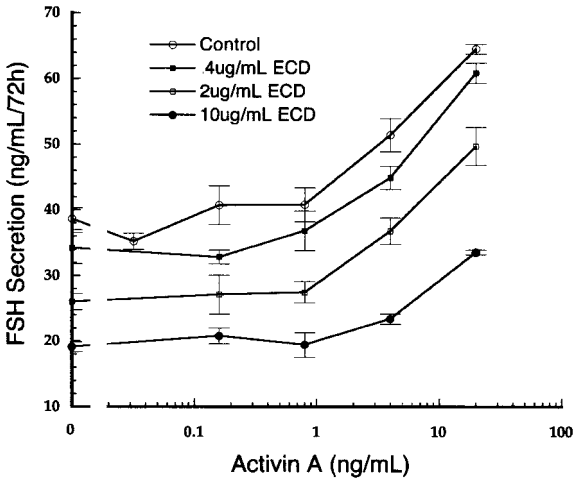

FIGURE 4: Results from the FSH release assay. Cells from the anterior pituitary glands of Sprague−Dawley rats were treated in triplicate with varying amounts of activin A and ActRII-dg. The level of FSH released was measured after 72 h.

activin signaling, acting most likely by sequestering activin away from full-length membrane-bound ActRII. Furthermore, ActRII-dg does not cause any change in ACTH release (data not shown), providing evidence for a receptor-specific signaling inhibition.

Stoichiometry of the Complex. The size of the complex between ActRII-ECD and activin A was first measured by gel filtration. The complex eluted at a calculated mass of 35 kDa, suggesting that the complex is formed by one activin dimer binding to one ActRII-ECD. The gel filtration was carried out by injecting a mixture of activin A and ActRII-ECD with an excess of receptor so that the predominant species in solution are the complex and unliganded receptor. The chromatograms from the gel filtration with and without activin A are shown in Figure 2C,D. Due to the potentially large errors in the masses estimated by gel filtration, more precise techniques were used to address the question of stoichiometry.

Cross-linking of radioactively labeled activin A to the ActRII-ECD resulted in the formation of two higher molecular mass species (Figure 5A). The molecular mass of these species as estimated by SDS−PAGE corresponds to activin A + 1 ActRII-ECD (∼37 kDa) and activin A + 2 ActRII-ECD (∼49 kDa). The cross-linking efficiency of DSS is generally low, on the order of 1−5%. It is therefore not surprising that the majority of the cross-linked material corresponds to the 1+1 complex. In a trimolecular reaction, the probability for the second cross-link to occur is much lower than that for the first one.

To accurately determine the stoichiometry of the complex, we performed equilibrium analytical ultracentrifugation on the complex which had been purified by gel filtration. The results show conclusively that the complex between ActRII-ECD and activin A consists of two ActRII-ECD molecules and one activin A dimer (Figure 5B). We also measured the sizes of ActRII-dg and ActRIIΔ14 which are both monomeric in solution (Figure 5C). The mass of the complex was measured to be 48.8 kDa, which is within experimental error of the calculated mass of 49.6 kDa. The masses of ActRII-dg and ActRIIΔ14 were measured to be 13.0 and 12.7 kDa, which is in good agreement with the calculated masses of 14.4 and 11.9 kDa, respectively. The data for the complex and for the receptor alone were fit to a two-species model, but in neither case did the fit improve significantly. This is the expected result for molecules that have nanomolar dissociation constants, because the small amount of uncomplexed material does not contribute to the signal more than the noise.

Crystallization. We obtained crystals of ActRIIΔ14 by the hanging-drop vapor diffusion method. The crystals grew in several conditions which were all in 0.1 M ammonium acetate buffer at pH 4.5. The best precipitants were either 5% PEG 8000 with 0.5 M NaCl, or 20% MPD, or 1 M ammonium sulfate. All conditions gave rise to hexagonal rod-shaped crystals. The crystals grew up to 500 × 200 × 200 μm and diffract X-rays beyond 2 Å. The crystals are in the space group *P3* and have the cell dimensions $a = b = 71.6$ Å $c = 37.3$ Å. Based on statistical comparison with other protein crystals (*27*), it is most probable that there are two molecules in the asymmetric unit, which would result in approximately a 43% solvent content.

DISCUSSION

There are two sites of potential glycosylation on ActRII, and in *P. pastoris*, these sites are both modified by mannose moieties which are attached to the asparagines by a two-*N*-

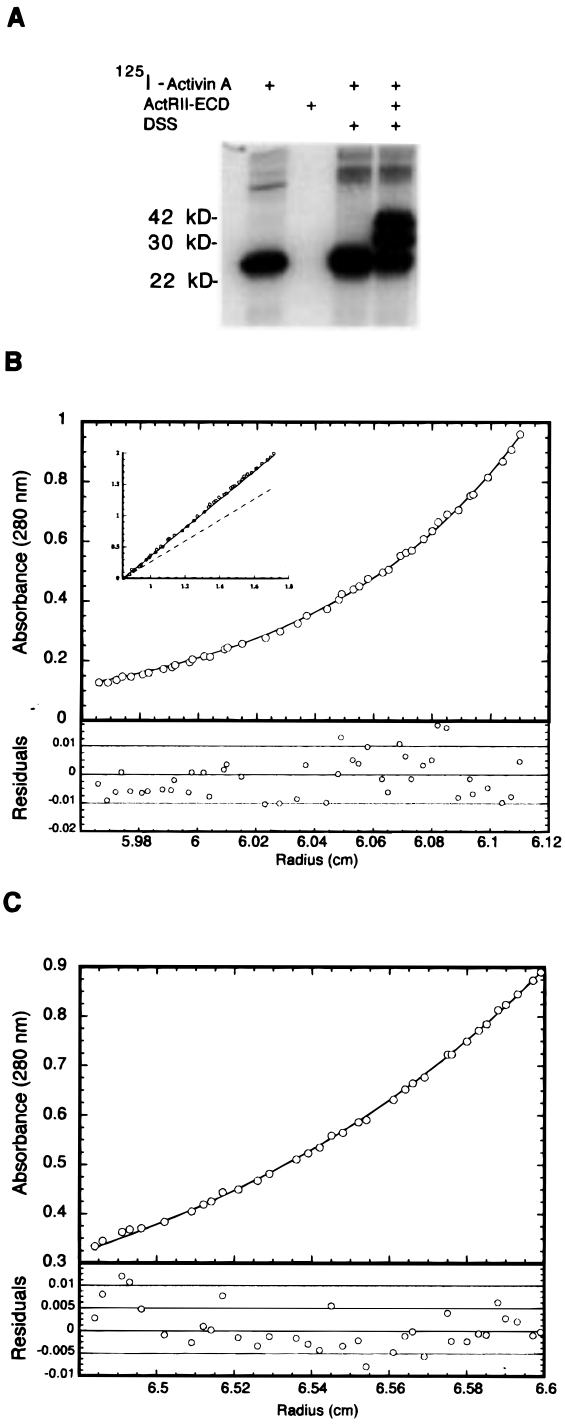

FIGURE 5: (A) Results from cross-linking of activin A and ActRII-ECD with disuccinimidyl suberate. The samples were visualized by SDS−PAGE and then exposure to X-ray film. The + above the lanes indicates which molecules were included in the reaction mixture. (B) Analytical ultracentrifuge data from a single speed (20k rpm) and concentration for the activin/ActRII-dg complex showing the global fit to all six data sets (14k and 20k rpm at 0.1, 0.2, and 0.4 mg/mL) and residuals for this fit. The inset graph shows the data plotted as the ln (concentration) + C versus ($r^2/2 - r_o^2/2$) where C is a constant added to have an x-intercept at the smallest r. The slope of the line is σ (see Experimental Procedures). The solid line is the gobal fit plotted in the same manner, and the dashed line is the expected model for a complex of one molecule of ActRII-dg with one activin A. (C) Analytical ultracentrifuge data from a single speed (28k rpm) and concentration for ActRII-dg showing the global fit to all six data sets (21k and 28k rpm at 0.15, 0.3, and 0.6 mg/mL) and residuals for this fit.

acetylglucosamine linker. Reported affinities of activin for its type II receptor range between 0.10 and 0.38 nM (*28*−*30*). The affinity for ActRII-ECD compared to intact cell receptors is thus reduced only 5-fold. A similar ratio has been reported for the affinity of TGFβ1 to the TGFβRII-ECD (*31*). In a different report on unglycosylated TGFβRII-ECD, a 1000-fold lower affinity is reported compared to intact cell surface receptors (*32*). The affinity of activin for the deglycosylated ActRII-ECD reported here is only about 25-fold lower. This indicates that the glycosylation is not essential for the high-affinity interaction between ActRII-ECD and activin A. Considering that the non-native mannose oligosaccharide from *P. pastoris* does not interfere with complex formation, it is reasonable to speculate that the binding surface is not near the glycosylation sites. We did not measure the mass of the glycosylated protein, but on SDS−PAGE, the sugars added about 5 kDa in mobility. Such large unnatural additions to the protein are likely to interfere with ligand binding if they are located close to the binding surface. Also, the 14 C-terminal residues which are missing in ActRIIΔ14 are not needed for complex formation.

The biological activity of ActRII-ECD, as measured in the FSH release asssay, fits within the current paradigm of the activin signaling mechanism. ActRII-ECD is likely to prevent signaling by binding to activin and impeding the formation of signaling complexes. The fact that a 1000-fold excess of ActRII-ECD to activin is required to effect these changes in FSH release could be attributed to several factors. First, the concentration of the receptors on the membrane is effectively higher than the calculated concentration because they are limited to a two-dimensional diffusion. Second, the length of the treatment (72 h) allows time for activin to be passed back and forth between soluble and membrane-bound receptors in an equilibrium manner. This will cause some signaling even at high ratios of ActRII-ECD:ActRII. Third, the cells express a basal level of activin, increasing the amount of activin that must be bound by ActRII-ECD to block signaling. Finally, it is possible that two ActRII-ECD molecules are needed to bind to activin in order to effectively block the signaling from the complex. If only one full-length receptor in the complex is sufficient to signal, the effective inhibition by the ECD alone will be weaker than expected for its K_D with activin.

The evidence for "ligand-induced receptor clustering" as the structural basis for the transmembrane signaling mechanism of receptor tyrosine kinases is extensive (*33*−*35*). However, the widespread occurrence of a homodimeric ligand (e.g., TGFβ family) interacting with heterodimeric receptor serine kinases raises the rarely discussed question of the relationship of the stoichiometry to the signaling mechanism for this class of receptors. Activin A presumably has a similar structure to the 2-fold symmetric TGFβ (*13*, *14*). The symmetry of the ligand and the stoichiometry of the activin/ActRII-ECD complex suggest that the complex is also structurally 2-fold symmetric. Although there is evidence for more than one type I receptor in the signaling complex (*36*), the question still remains as to how many type I receptors will be involved, but the symmetry argument still points toward two of each type of receptor in the ActRI/ActRII/activin complex. This type of ligand-mediated oligomerization supports the receptor-clustering model in which a type II receptor phosphorylates and activates a type I receptor; however, this model does not provide insight as to why nature has developed a heterodimeric ligand and receptor system. More detailed experiments on the kinetics of signaling in the presence of ActRII-ECD will shed light on this signaling mechanism.

ACKNOWLEDGMENT

We thank R. D. Mullins for help with the analytical ultracentrifuge data collection and also the NIDDK for supplying the activin A.

REFERENCES

1. McCarthy, S. A., and Bicknell, R. (1993) *J. Biol. Chem. 268*, 23066−23071.
2. Gonzalez-Manchon, C., and Vale, W. (1989) *Endocrinology 125*, 1666−1672.
3. Ogawa, Y., Schmidt, D. K., Nathan, R. M., Armstrong, R. M., Miller, K. L., Sawamura, S. J., Ziman, J. M., Erickson, K. L., de Leon, E. R., Rosen, D. M., Seyedin, S. M., Glaser, C. B., Chang, R. J., Corrigan, A. Z., and Vale, W. (1992) *J. Biol. Chem. 267*, 14233−14237.
4. Mitrani, E., Ziv, T., Thomsen, G., Shimoni, Y., Melton, D. A., and Bril, A. (1990) *Cell 63*, 495−501.
5. Green, J. B., and Smith, J. C. (1990) *Nature 347*, 391−394.
6. Vale, W., Rivier, J., Vaughan, J., McClintock, R., Corrigan, A., Woo, W., Karr, D., and Spiess, J. (1986) *Nature 321*, 776−779.
7. Petraglia, F., Vaughan, J., and Vale, W. (1989) *Proc. Natl. Acad. Sci. U.S.A. 86*, 5114−5117.
8. Farnworth, P. G., Robertson, D. M., de Kretser, D. M., and Burger, H. G. (1988) *J. Endocrinol. 119*, 233−241.
9. Fang, J., Yin, W., Smiley, E., Wang, S. Q., and Bonadio, J. (1996) *Biochem. Biophys. Res. Commun. 228*, 669−674.
10. Fang, J., Wang, S. Q., Smiley, E., and Bonadio, J. (1997) *Biochem. Biophys. Res. Commun. 231*, 655−661.
11. Hotten, G., Neidhardt, H., Schneider, C., and Pohl, J. (1995) *Biochem. Biophys. Res. Commun. 206*, 608−613.
12. Oda, S., Nishimatsu, S., Murakami, K., and Ueno, N. (1995) *Biochem. Biophys. Res. Commun. 210*, 581−588.
13. Daopin, S., Piez, K. A., Ogawa, Y., and Davies, D. R. (1992) *Science 257*, 369−373.
14. Schlunegger, M. P., and Grütter, M. G. (1992) *Nature 358*, 430−434.
15. Boyd, F. T., and Massague, J. (1989) *J. Biol. Chem. 264*, 2272−2278.
16. Wrana, J. L., Attisano, L., Carcamo, J., Zentella, A., Doody, J., Laiho, M., Wang, X. F., and Massague, J. (1992) *Cell 71*, 1003−1014.
17. Mathews, L. S., and Vale, W. W. (1991) *Cell 65*, 973−982.
18. Wrana, J. L., Tran, H., Attisano, L., Arora, K., Childs, S. R., Massague, J., and O'Connor, M. B. (1994) *Mol. Cell. Biol. 14*, 944−950.
19. Wieser, R., Wrana, J. L., and Massague, J. (1995) *EMBO J. 14*, 2199−2208.
20. Franzen, P., Heldin, C. H., and Miyazono, K. (1995) *Biochem. Biophys. Res. Commun. 207*, 682−689.
21. Wrana, J. L., Attisano, L., Wieser, R., Ventura, F., and Massague, J. (1994) *Nature 370*, 341−347.
22. Cregg, J. M., Barringer, K. J., Hessler, A. Y., and Madden, K. R. (1985) *Mol. Cell. Biol. 5*, 3376−3385.
23. Sreekrishna, K., Tschopp, J. F., and Fuke, M. (1987) *Gene 59*, 115−125.
24. Scorer, C. A., Clare, J. J., McCombie, W. R., Romanos, M. A., and Sreekrishna, K. (1994) *Bio/Technology 12*, 181−184.
25. Johnson, M. L., Correia, J. J., Yphantis, D. A., and Halvorson, H. R. (1981) *Biophys. J. 36*, 575−588.
26. Clare, J. J., Rayment, F. B., Ballantine, S. P., Sreekrishna, K., and Romanos, M. A. (1991) *Bio/Technology 9*, 455−460.
27. Matthews, B. W. (1968) *J. Mol. Biol. 33*, 491−497.

28. Donaldson, C. J., Mathews, L. S., and Vale, W. W. (1992) *Biochem. Biophys. Res. Commun. 184*, 310−316.
29. Campen, C. A., and Vale, W. (1988) *Biochem. Biophys. Res. Commun. 157*, 844−849.
30. Attisano, L., Wrana, J. L., Cheifetz, S., and Massague, J. (1992) *Cell 68*, 97−108.
31. Lin, H. Y., Moustakas, A., Knaus, P., Wells, R. G., Henis, Y. I., and Lodish, H. F. (1995) *J. Biol. Chem. 270*, 2747−2754.
32. Goetschy, J. F., Letourneur, O., Cerletti, N., and Horisberger, M. A. (1996) *Eur. J. Biochem. 241*, 355−362.
33. Banner, D. W., D'Arcy, A., Janes, W., Gentz, R., Schoenfeld, H. J., Broger, C., Loetscher, H., and Lesslauer, W. (1993) *Cell 73*, 431−445.
34. DeVos, A. M., Ultsch, M., and Kossiakoff, A. A. (1992) *Science 255*, 306−312.
35. Ullrich, A., and Schlessinger, J. (1990) *Cell 61*, 203−212.
36. Weis-Garcia, F., and Massague, J. (1996) *EMBO J. 15*, 276−289.

BI981939O